TFD Element Efficiency Analysis

Dave Typinski
Typinski Radio Astronomy, Inc.
January, 2020

Spectrograph Users Group (SUG) stations endeavor to provide scientifically useful observation data. To achieve this goal, emission amplitude measurement is required. An important component of amplitude calculation is antenna array element efficiency across the portion of the spectrum being observed. This work analyzes and provides a model of 24′ and 30′ terminated folded dipole (TFD) element efficiencies over poor natural ground from 14 to 33 MHz.

The TFD Array

The Typinski Radio Astronomy (TRA) AN-TFD-24-4 antenna array is a wideband upper-HF band antenna array used by SUG stations to provide RCP and LCP signals to spectrographs. The array is constructed of four 24-foot terminated folded dipole (TFD) elements arranged in a square.[1] Some stations operate TFD arrays with 30-foot elements and some stations operate eight-element arrays (two four-element squares).[2]

The terminated folded dipole design has a wide bandwidth at the expense of a lossy response.

The IEEE definition of radiation efficiency is "The ratio of the total power radiated by an antenna to the net power accepted by the antenna from the connected transmitter."[3] By the principle of reciprocity, we define the efficiency of the TFD element slightly differently as the ratio of the power accepted by a 50 Ω load from the TFD balun to the total power accepted by a 50 Ω load from the feed point of a perfectly matched ½λ dipole antenna.

The efficiency of the TFD element varies with frequency and is due to losses in the termination resistor, the folded design of the element wire, losses within the balun, and loss from the impedance mismatch between the balun and feed line.

Prior Work

Measurements of the 24′ and 30′ TFD efficiencies relative to a 20.1 MHz Radio JOVE dipole were made in August, 2014. That test used a Radio JOVE receiver to record the 20.1 MHz galactic background (GB) for three days for each antenna (reference half wave dipole, 24′ TFD, and 30′ TFD) one after the other with the hope that ionospheric attenuation didn't vary between GB measurements. The results of that analysis were:

-3.2 dB 20 MHz efficiency for the 30′ TFD and -4.3 dB 20 MHz efficiency for the 24′ TFD.

That test program was not carried out at any other radio frequency. Data analysis used a measured balun loss of ~ 0.5 dB; however, the present work does not make that assumption. The measured balun loss is valid only when the balun is terminated with 800+j0 Ω (high-Z side) and 50+ j0 Ω (low-Z side) impedances constant across the RF spectrum. That is, the constant-with-frequency 800 + j0 Ω high-Z condition does not exist when the balun is connected to a TFD wire element.

Equipment

An antenna test range was temporarily provisioned at AJ4CO Observatory in place of the riometer array. The range consisted of a reference half-wave dipole and a TFD as shown in Fig. 1. Both antennas had element arms

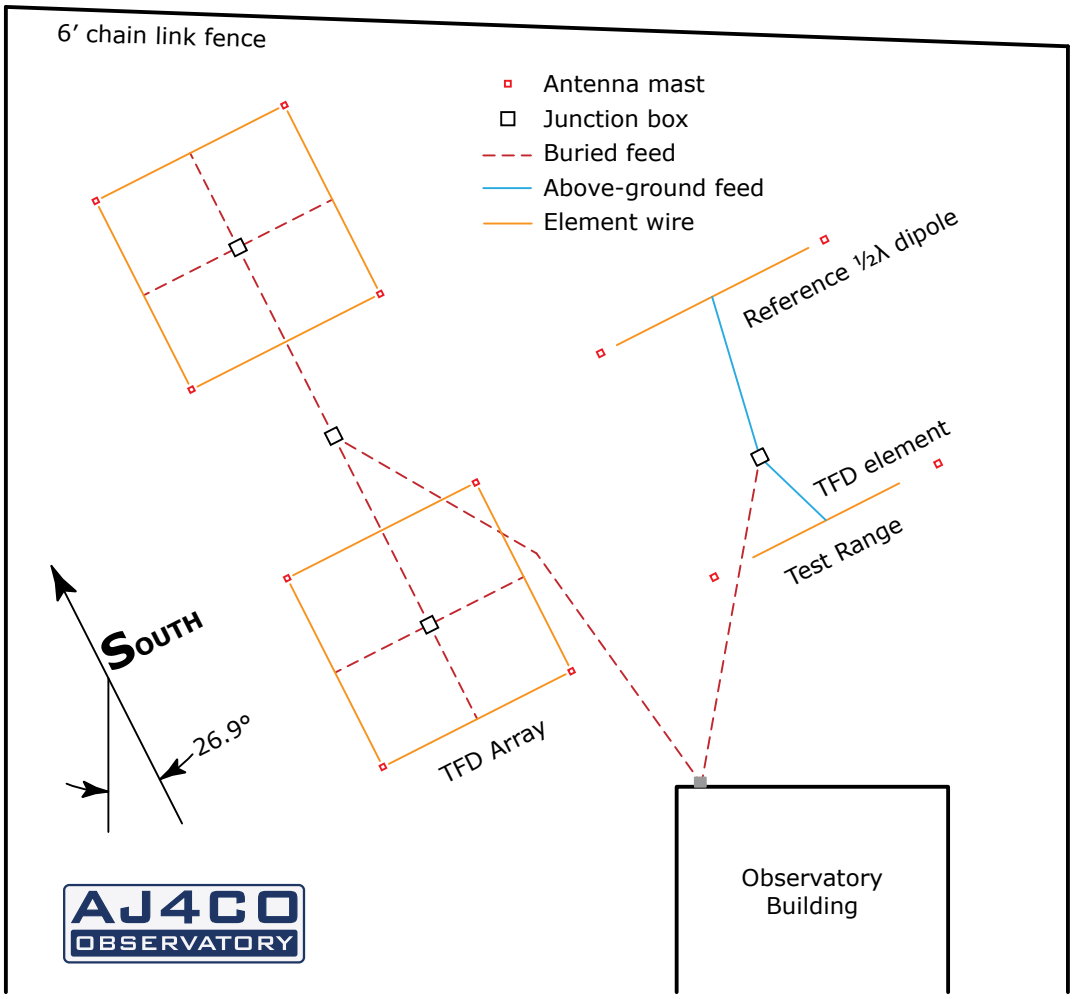

Figure 1 – Test range layout.

running east-west with a 38 foot north-south separation between the two antennas. This spacing evenly split the available distance between the observatory building and a chain link fence at the south side of the property.

Both antennas were installed over natural ground (no ground screen) as this is how they are installed at SUG observatories. We note that variations in ground conditions may cause the efficiency of the TFD array to vary from station to station.

A reference dipole (see Fig. 2) was fabricated to be resonant at 14 MHz and was trimmed every other day one MHz shorter. On the days the reference dipole was not trimmed, the TFD element (see Fig. 3) was swapped from 24′ to 30′ and vice versa. Thus, both TFD lengths were tested at all measurement radio frequencies. See Appendix 3.

All feed lines were characterized from 10 to 40 MHz using a two-port vector network analyzer (VNA). The feeds for the reference dipole and the TFD element contained 14-bead (Fair-Rite P/N 2631480002) common mode

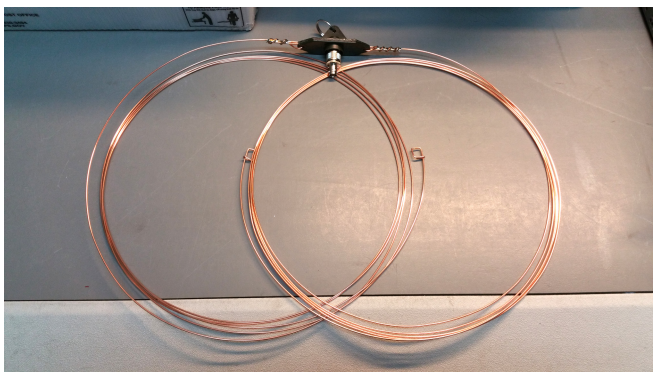

Figure 2 – The 14 MHz reference dipole; 14 guage copper clad steel (Wireman # 502).

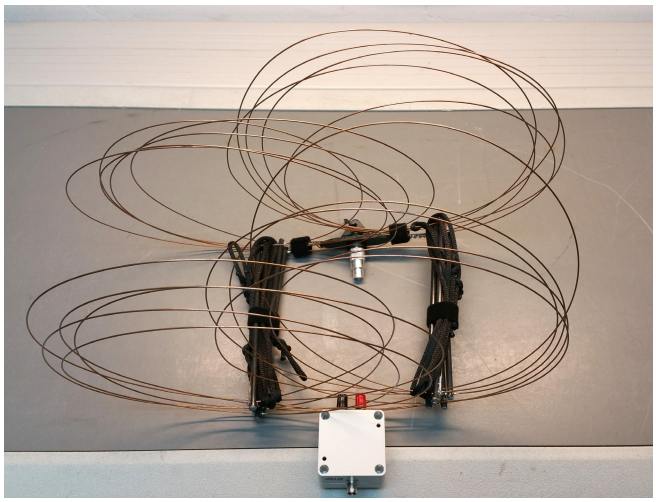

Figure 3 – The 30′ TFD element coiled for storage.[1]

chokes at the feed point ends of the feed lines (see Fig. 4).

Each antenna fed an Icom R75 receiver configured as a radiometer. For some of the test frequencies, the R75s were preceded by a matched pair of 17 to 34 MHz band pass filters and 16 dB preamplifiers. See Appendices 7 through 14.

The AJ4CO Automatic Calibrator was modified for this test program by the addition of Mini-Circuits coaxial pads immediately after the internal noise source.[4] This brought the calibration steps colder, providing more calibration steps at the weaker signal levels expected from the TFD elements at the higher test frequencies. See Appendix 9.

The Automatic Calibrator components were characterized over the 10 to 40 MHz range using a two-port VNA to measure losses and a spectrum analyzer to profile the internal noise source's output spectrum. The noise source's 20 MHz output was measured at 430 MK ± 0.1 dB using a 5722 lab standard on 05 Jan 2020. See Appendix 10.

Method

As in the prior test, the present work assumes the radiation efficiency of a half wave dipole

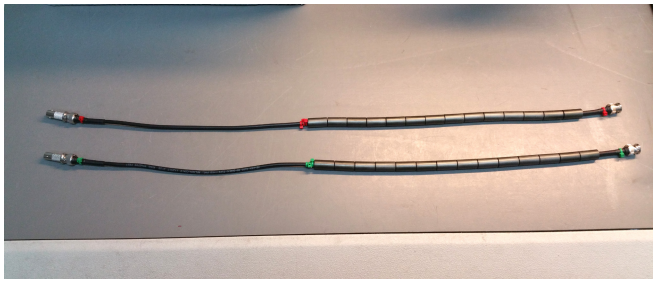

Figure 4 – Common mode chokes for feed point ends of feed lines.

operated at its resonant frequency is 100%, making it the ideal reference antenna.

The noise temperatures of the GB observed using TFD elements and a reference dipole were measured when the galactic plane was furthest from zenith (i.e., when the coldest antenna temperatures were observed) to minimize the effect of the slight difference in beam shape between the half-wave dipole and the TFD (see Appendix 4). Beam shape does not affect antenna temperature if the emission source is uniform across the sky, a condition loosely approximated for a single dipole in the upper HF band when the galactic plane is at low elevation angles.

The half-wave reference dipoles were trimmed every 1 MHz. Wire heights were adjusted to maintain 0.20 ± 0.03 λ above ground. Feed point characteristics were measured using a VNA after each change. The TFD element balun output characteristics were also measured. See Appendices 1, 5, and 6.

Data Analysis

Each antenna's GB antenna temperature measurement was calibrated by weighted average double parabolic interpolation from the array of 50-second averages of known equivalent antenna temperatures in a step calibration performed within two hours of each GB measurement.

Equivalent antenna temperatures for each antenna (TFD and reference dipole) were

calculated for each step of the calibration via Equation 1. See Appendices 7 and 8 for feed system losses.

$$T_{ant} = 10^{\left(\frac{L_{feed}}{10}\right)}\left[T_{cp} - T_0\left(1 - 10^{\left(\frac{L_{feed}}{10}\right)}\right)\right] \quad (1)$$

where

T_{ant} = equivalent noise temperature at antenna feed point.
T_0 = 290 K.
T_{cp} = noise temperature at calibration plane.
L_{feed} = feed system loss between feed point and calibration plane in terms of decibels.

The interpolated GB antenna temperatures of the reference dipole were then corrected by accounting for the losses due to the measured impedance mismatch with respect to a 50 Ω system via Equations 2 and 3. This correction assumes the receiver presents a perfect (non-reactive) 50 Ω load to the feed line. See Appendix 2.

$$L_{mismatch(dB)} = 10\log\left[1 - \rho^2\right] \quad (2)$$

$$T_{corrected} = T_{ant}\,10^{\left(\frac{L_{mismatch(dB)}}{10}\right)} \quad (3)$$

where

ρ = vector magnitude of feed point reflection coefficient (provided by VNA measurement).

Loss due to the TFD balun output impedance mismatch with the feed line is considered part of the TFD antenna efficiency and not accounted for separately.

The efficiencies of the TFD elements with respect to a perfectly impedance-matched half wave dipole were determined by comparing the measured temperatures from the TFD elements to the corrected temperatures from the reference dipoles via Equation 4.

$$\eta_{TFD} = 10\log\left(\frac{T_{ant\ (TFD)}}{T_{corrected\ (reference\ dipole)}}\right) \quad (4)$$

Results

The results of the data analysis are shown in Table 1, Table2, Plot 1, and Plot 2.

Quartic curves were fitted to the TFD efficiency data via polynomial regression using Origin 9 software, resulting in equations 5 and 6. These equations enable conversion of observed TFD feed point (balun output) temperatures to sky-side antenna temperatures (i.e., ½λ-dipole-equivalent temperatures) for frequencies between 14 and 33 MHz.

$$\eta_{24'TFD} = -4.223\times10^{-5} f^4 + 4.863\times10^{-3} f^3 - 0.2660 f^2 + 7.116 f - 7.388 \quad (5)$$

$$\eta_{30'TFD} = -6.699\times10^{-4} f^4 + 6.658\times10^{-2} f^3 - 2.449 f^2 + 39.50 f - 240.6 \quad (6)$$

where

η = efficiency in terms of decibels.
f = frequency in MHz, $14 \le f \le 33$.

Acknowledgement

This work was funded in part by NASA NSSEC / HEC grant number NNX16AL49A to Middle Tennessee State University.

References

[1] Typinski, *TRA AN-TFD-24-4 Square Array Manual*, TRA (2020).

[2] *Station Diagrams*, SUG (2019).

[3] IEEE Standard 145-1993, *Standard Definitions of Terms for Antennas*, IEEE (1993)

[4] Typinski, *AJ4CO Automatic Calibrator*, AJ4CO (2017).

[5] Typinski, *The Galactic Background in the Upper HF Band*, AJ4CO (2013).

Freq (MHz)	Reference ½λ Dipole $T_{corrected}$ (kK)	24′ TFD Output Into 50Ω T_{ant} (kK)	Raw 24′ TFD Efficiency Relative to Perfectly Matched ½λ Dipole (dB)	Reference ½λ Dipole $T_{corrected}$ (kK)	30′ TFD Output Into 50Ω T_{ant} (kK)	Raw 30′ TFD Efficiency Relative to Perfectly Matched ½λ Dipole (dB)
14.4	67	2.8	-14	59	6.8	-9.4
15.1	52	2.5	-13	51	6.7	-8.8
16.1	43	4.9	-9.4	41	10	-6.1
17.1	34	3.6	-9.7	44	11	-6.0
18.0	32	4.4	-8.6	31	8.8	-5.6
19.1	29	5.4	-7.3	29	8.9	-5.2
20.1	24	6.5	-5.6	24	8.8	-4.4
21.0	23	7.7	-4.7	22	8.0	-4.3
22.1	24	9.8	-3.9	24	7.5	-5.0
23.1	20	8.8	-3.6	19	6.1	-4.9
24.1	15	9.3	-2.1	16	4.0	-6.1
25.1	14	7.0	-2.9	14	5.4	-4.1
26.1	13	6.2	-3.3	13	3.5	-5.7
27.1	11	6.1	-2.5	11	3.3	-5.4
28.1	11	6.5	-2.5	12	3.4	-5.3
29.1	9.8	5.8	-2.3	10	3.9	-4.1
30.1	8.4	4.7	-2.5	8.3	2.8	-4.7
31.1	8.2	4.3	-2.8	8.3	3.0	-4.4
32.1	8.1	3.4	-3.8	8.2	2.2	-5.7
33.1	8.6	3.3	-4.1	8.4	2.1	-6.0

Table 1 – Raw TFD element efficiencies relative to a perfectly matched ½λ dipole. The efficiencies shown here include all losses between the sky side of the TFD antenna and the feed point end of the feed line.

$$\eta_{24'TFD} = -4.223\times10^{-5} f^4 + 4.863\times10^{-3} f^3 - 0.2660 f^2 + 7.116 f - 7.388$$

$$\eta_{30'TFD} = -6.699\times10^{-4} f^4 + 6.658\times10^{-2} f^3 - 2.449 f^2 + 39.50 f - 240.6$$

Freq (MHz)	24′ TFD Efficiency Relative to Perfectly Matched ½λ Dipole (dB)	30′ TFD Efficiency Relative to Perfectly Matched ½λ Dipole (dB)
14	-15	-11
15	-13	-8.4
16	-11	-6.8
17	-9.4	-5.8
18	-8.0	-5.2
19	-6.8	-4.9
20	-5.8	-4.8
21	-4.9	-4.9
22	-4.2	-5.0
23	-3.6	-5.1
24	-3.1	-5.2
25	-2.7	-5.2
26	-2.5	-5.1
27	-2.4	-5.0
28	-2.4	-4.9
29	-2.5	-4.8
30	-2.7	-4.7
31	-3.0	-4.9
32	-3.5	-5.2
33	-4.0	-5.9

Table 2 – Quartic curve fits to raw TFD efficiencies. The efficiencies shown here include all losses between the sky side of the TFD antenna and the feed point end of the feed line.

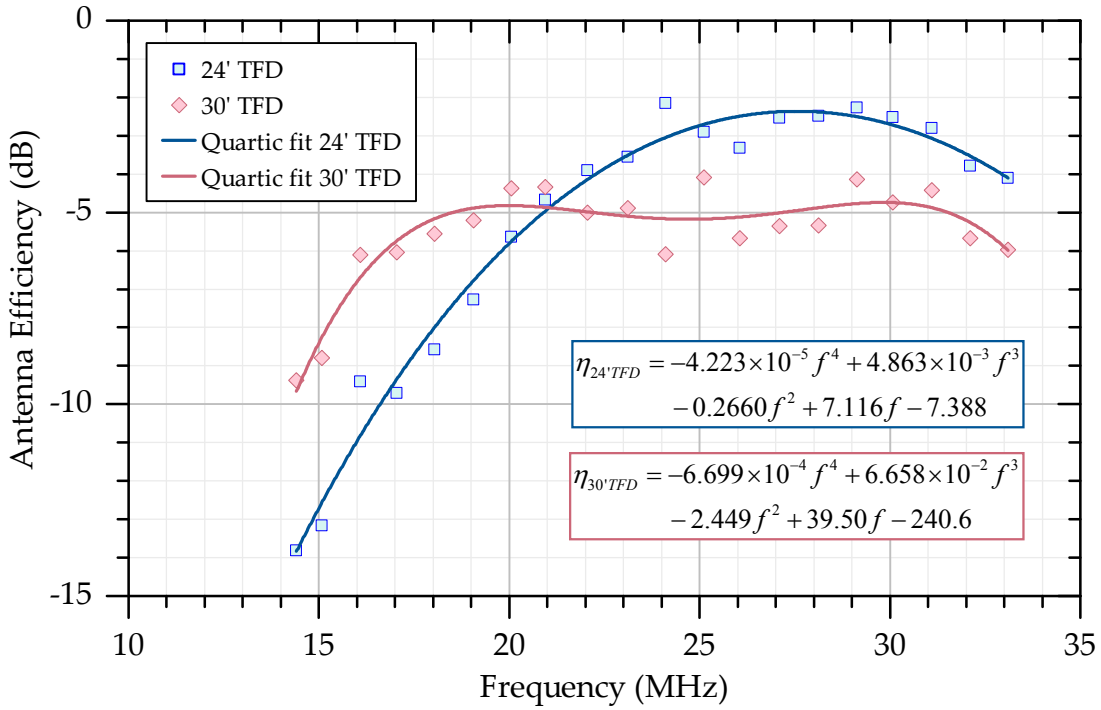

Plot 1 – Measured TFD element efficiencies relative to a perfectly matched ½λ dipole. The efficiencies shown here includes all losses between the sky side of the TFD antenna and the feed point end of the feed line.

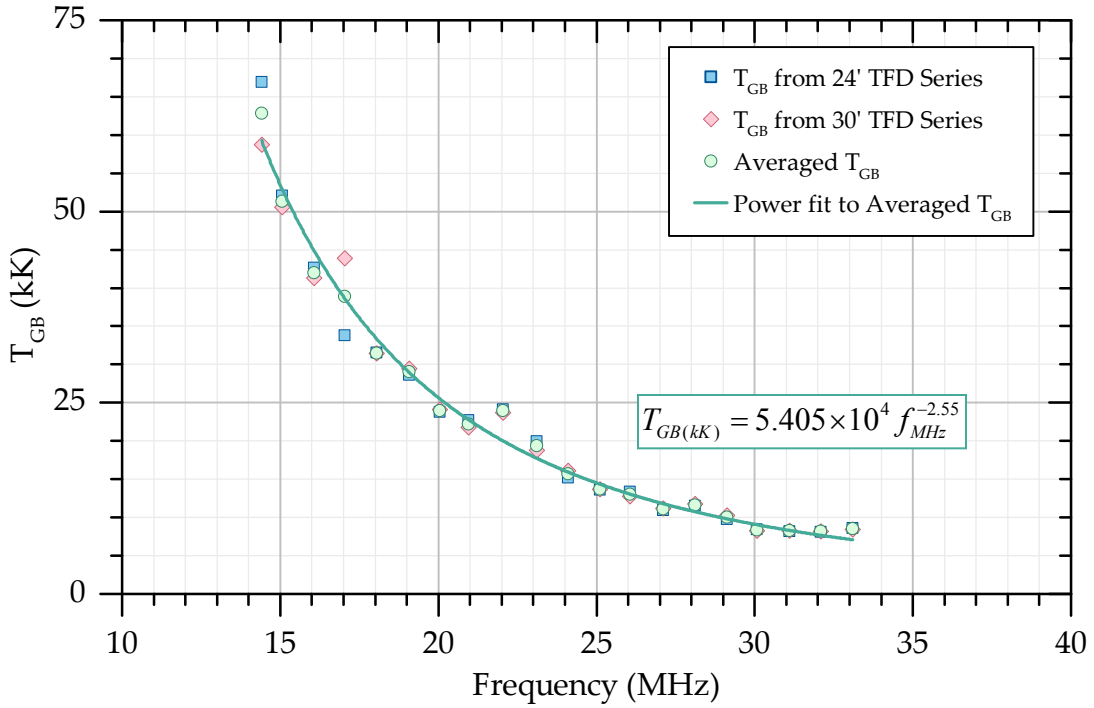

Plot 2 – Galactic background (GB) antenna temperatures measured using the reference dipoles. One series represents measurements used for comparison with the 24′ TFD, the other represents measurements used for comparison with the 30′ TFD. The series were averaged at each frequency and a power function fitted to the averages using Origin 9 software. The result shows a spectral index of -2.55 and a 20 MHz antenna temperature of 26 kK. The measured noise temperature of the GB is thus 52 kK because the GB emission is randomly polarized. An antenna can only receive half the available radiation in randomly polarized emission (this is true regardless of whether the antenna is linearly or circularly polarized). The known spectral index of the polar galactic background is -2.56 and the known 20 MHz temperature of the galactic background is 50 kK.[5] Close agreement with the accepted values shows that the impact of any radio frequency interference (RFI) on the efficiency analysis as a whole is not significant, RFI being expected to have a spectrum different than that of the GB and to cause measured temperatures to be hotter than the GB alone. RFI may have had an impact at individual test frequency measurements, but none appear to have been greatly affected by RFI.

APPENDICES

Appendix 1 – Reference Dipole Dimensions and Feed Point S_{11} ◊

Nominal Freq (MHz)	Wire Length (ft-in)	Wire Height Over Natural Ground † (ft-in)	($\lambda_{K=0.95}$)	Resonant Freq ‡ (MHz)	Minimum |Z| Freq (MHz)	Minimum |Z| (Ω)	Minimum SWR Freq (MHz)	Minimum SWR (50 Ω)
14.1	33' 5-1/4"	14' 9"	0.21	14.19	14.08	73	14.17	1.48
15.1	31' 2-3/4"	14' 9"	0.22	15.19	15.08	74	15.13	1.49
16.1	29' 3-1/2"	12' 2"	0.20	16.19	16.07	70	16.17	1.43
17.1	27' 6-3/4"	12' 2"	0.21	17.18	17.03	70	17.15	1.42
18.1	26' 0-1/2"	12' 2"	0.22	18.16	17.93	69	18.11	1.40
19.1	24' 8-1/4"	12' 2"	0.23	19.15	18.99	70	19.10	1.42
20.1	23' 6-1/2"	9' 10"	0.20	20.06	19.92	64	20.03	1.30
21.1	22' 5-1/4"	9' 10"	0.21	21.04	20.89	65	21.00	1.32
22.1	21' 2-1/4"	9' 5"	0.21	22.08	21.87	68	22.02	1.38
23.1	20' 4"	8' 8"	0.20	23.25	23.01	65	23.15	1.33
24.1	19' 7-1/4"	8' 8"	0.21	24.26	24.08	67	24.21	1.37
25.1	18' 8-1/4"	8' 0"	0.20	25.19	24.92	65	25.13	1.33
26.1	18' 0-3/4"	8' 0"	0.21	26.05	25.75	67	25.96	1.37
27.1	17' 2-3/4"	6' 6"	0.18	27.18	26.93	62	27.10	1.27
28.1	16' 7-1/2"	6' 6"	0.19	28.26	28.00	68	28.21	1.29
29.1	16' 1-1/2"	6' 6"	0.19	29.15	28.88	64	29.09	1.31
30.1	15' 7"	6' 6"	0.20	30.11	29.81	66	30.03	1.35
31.1	15' 0-1/2"	6' 6"	0.21	31.20	30.83	67	31.12	1.36
32.1	14' 7"	6' 6"	0.21	32.18	31.83	68	32.08	1.39
33.1	14' 1-1/2"	6' 6"	0.22	33.17	32.75	69	33.08	1.40

◊ S_{11} values measured with an Array Solutions VNA-2180 VNA calibrated to the feed point end of the feed line.

† Height in terms of wavelengths caculated from height/λ where $\lambda = 2l/k$ where l = dipole wire length and $k = 0.95$ to account for the velocity of propagation within the dipole wire arising from end effect.

‡ Resonance occurs when the feed point impedance is purely resistive; i.e., the frequency at which reactance X = 0 Ω.

Freq (MHz)	S_{11} at Frequency Used for GB Observation ◊ R (Ω)	X (Ω)	|Z| (Ω)	ρ (50 Ω)	SWR (50 Ω)	Mismatch Loss (dB)	For 24' TFD Comparison Measured T_{ant} (kK)	Calculated $T_{corrected}$ (kK)	For 30' TFD Comparison Measured T_{ant} (kK)	Calculated $T_{corrected}$ (kK)
14.41	78.7	23.0	82.0	0.281	1.78	-0.36	62	67	54	59
15.07	72.8	-11.9	73.8	0.209	1.53	-0.19	50	52	48	51
16.08	69.7	-10.6	70.5	0.186	1.46	-0.15	41	43	40	41
17.05	69.4	-11.7	70.4	0.189	1.47	-0.16	33	34	42	44
18.04	68.4	-9.5	69.1	0.174	1.42	-0.13	31	32	31	32
19.07	70.5	-5.6	70.7	0.176	1.43	-0.14	28	29	29	29
20.05	65.5	-0.6	65.5	0.134	1.31	-0.08	23	24	24	24
20.95	64.9	-6.0	65.2	0.140	1.33	-0.09	22	23	21	22
22.05	69.0	-2.1	69.0	0.160	1.38	-0.11	24	24	23	24
23.11	65.0	-8.4	65.5	0.149	1.35	-0.10	20	20	18	19
24.10	66.2	-9.8	66.9	0.162	1.39	-0.12	15	15	16	16
25.12	66.3	-4.0	66.4	0.144	1.34	-0.09	13	14	13	14
26.05	68.9	0.3	68.9	0.159	1.38	-0.11	13	13	12	13
27.10	62.8	-3.9	62.9	0.119	1.27	-0.06	11	11	11	11
28.12	63.5	-7.2	63.9	0.135	1.31	-0.08	11	12	12	12
29.13	65.8	-1.1	65.8	0.137	1.32	-0.08	10	9.8	10	10
30.07	67.4	-1.8	67.4	0.149	1.35	-0.10	8.2	8.4	8.1	8.3
31.10	67.5	-4.7	67.6	0.154	1.36	-0.10	8.0	8.2	8.1	8.3
32.10	68.9	-3.2	69.0	0.161	1.38	-0.11	7.9	8.1	8.0	8.2
33.10	70.2	-2.4	70.2	0.169	1.41	-0.13	8.4	8.6	8.2	8.4

◊ S_{11} values measured with an Array Solutions VNA-2180 VNA calibrated to the feed point end of the feed line.

Appendix 3 – TFD Dimensions

Antenna	Element Length (ft-in)	Top Wire Height (ft-in)
24′ TFD	24′ 0″	9′ 2″
30′ TFD	30′ 0″	9′ 2″

Appendix 4 – Antenna Beam Patterns

From EZNEC models. Antenna dimensions per Appendices 1 and 3.

20.1 MHz ½λ reference dipole beam pattern modeled above poor ground. Azimuth pattern at 45° elevation. Patterns representative of all reference dipoles used.

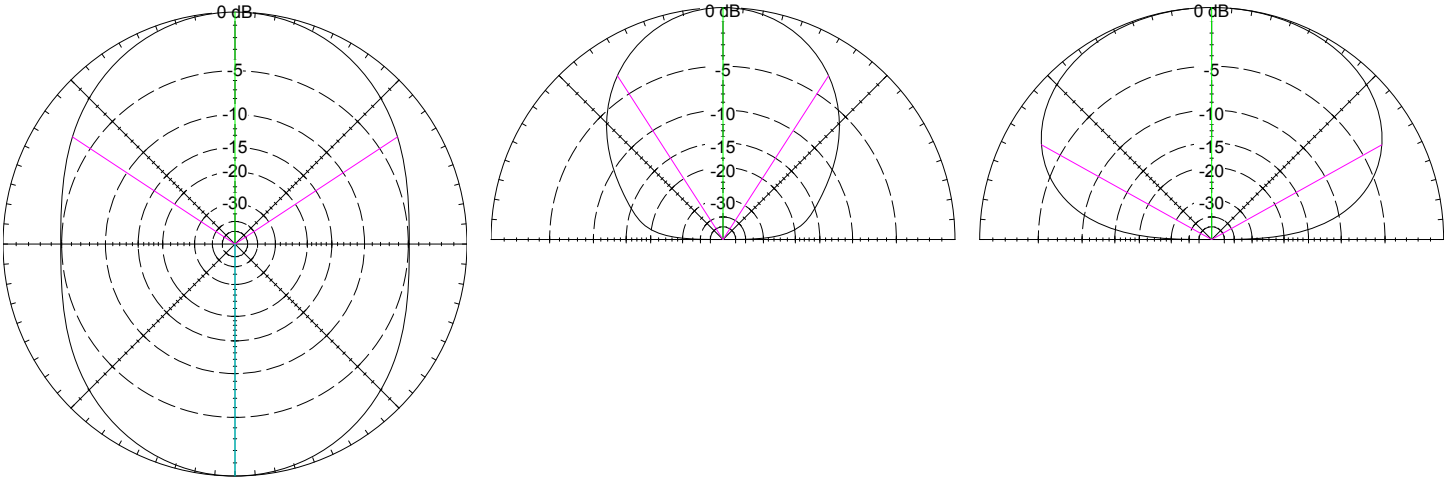

24′ TFD 20.1 MHz beam pattern modeled above poor ground. Azimuth pattern at 45° elevation.

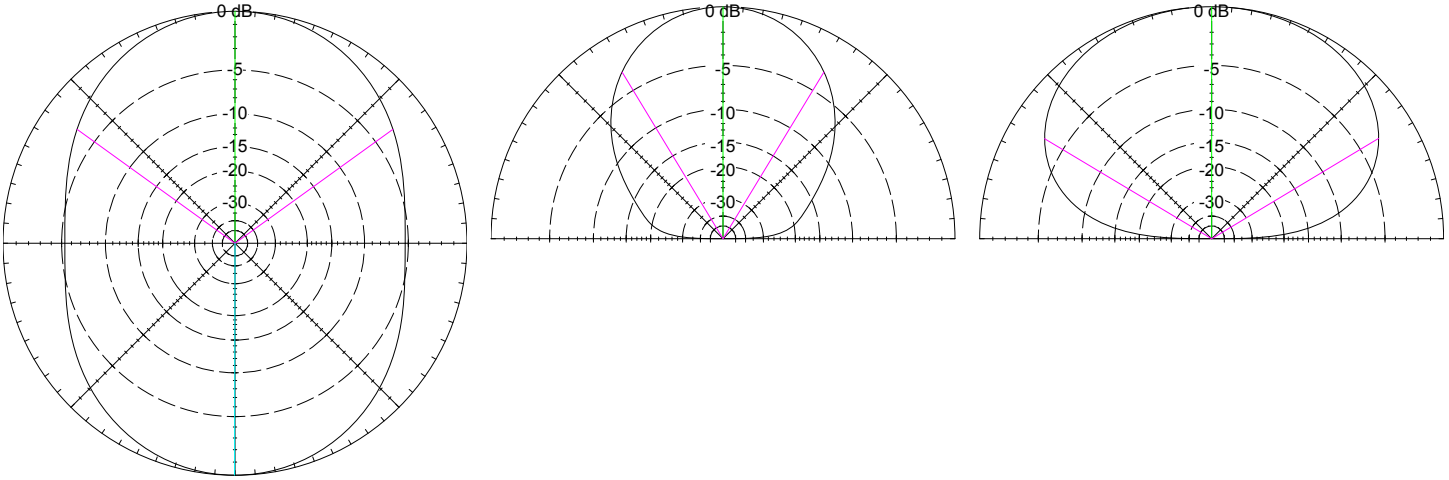

30′ TFD 20.1 MHz beam pattern modeled above poor ground. Azimuth pattern at 45° elevation.

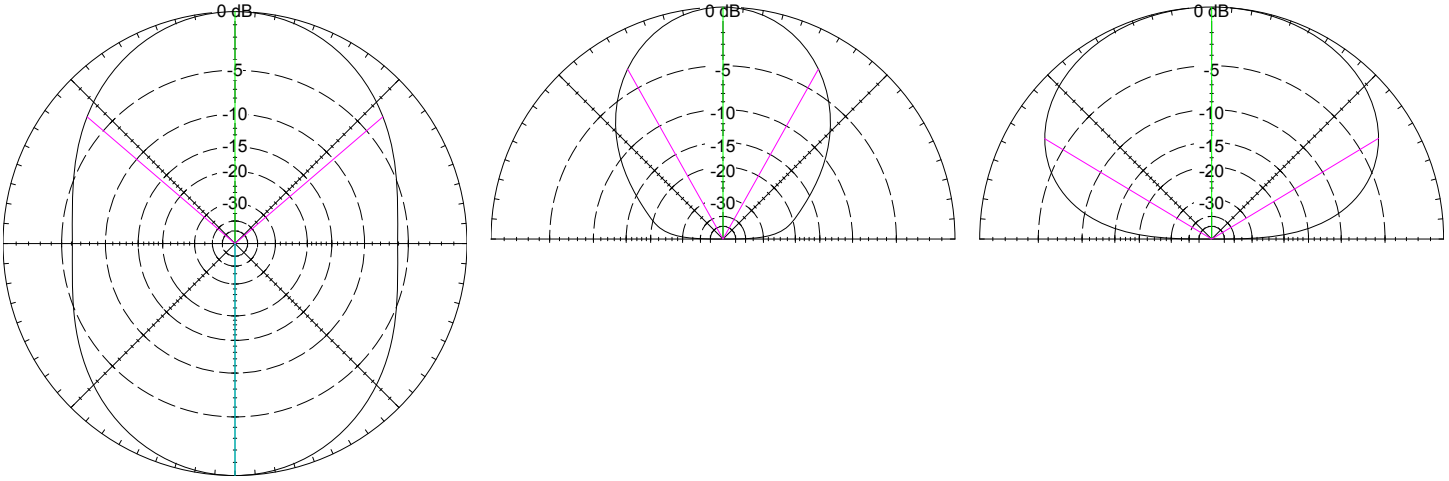

Appendix 5 – Reference Dipole Feed Point Characteristics Plots

Measured above natural ground (no ground screen).

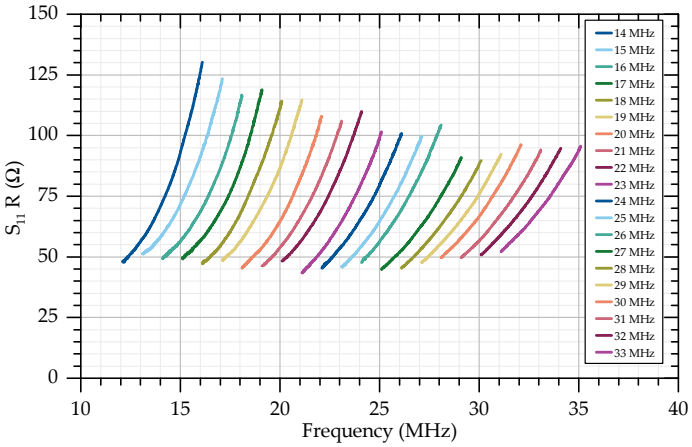

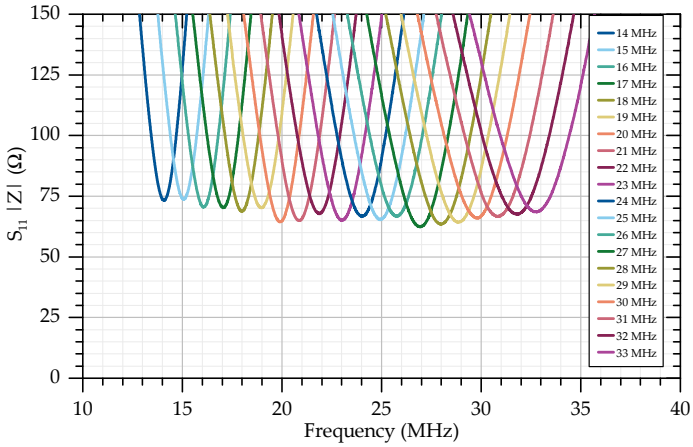

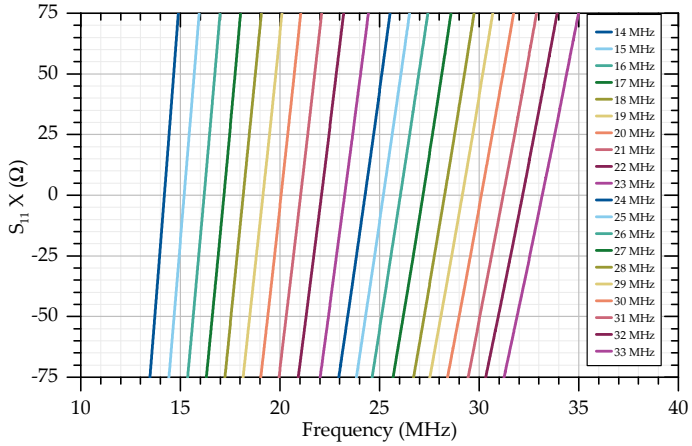

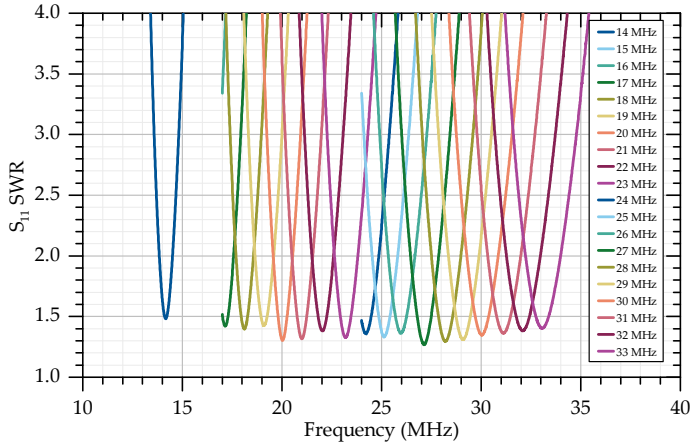

Appendix 6 – TFD Element Feed Point (Balun Output) Characteristics Plots

Measured above natural ground (no ground screen).

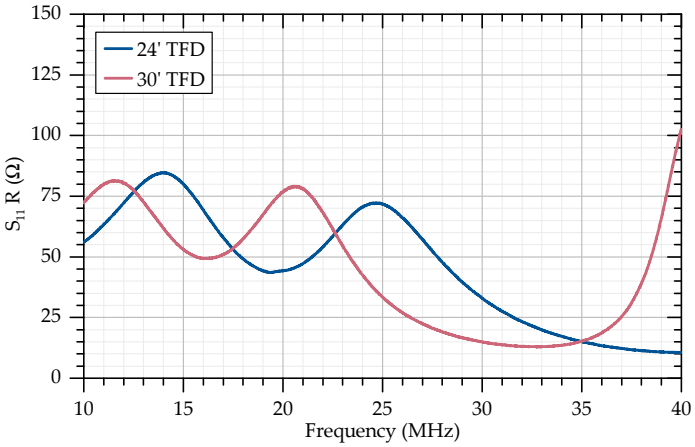

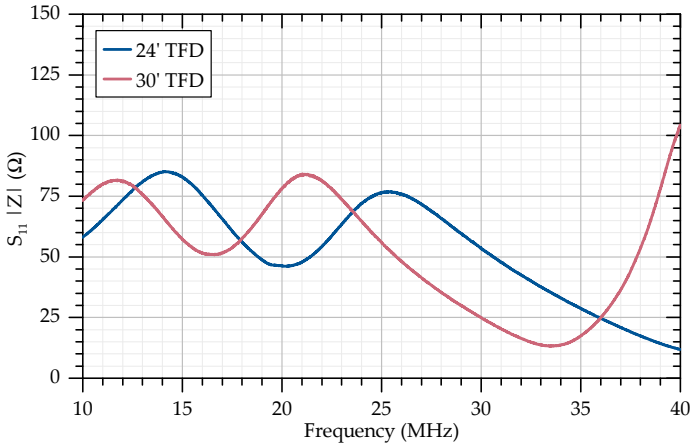

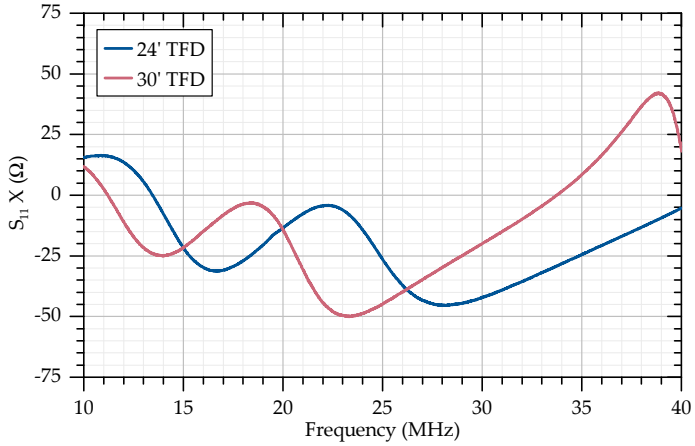

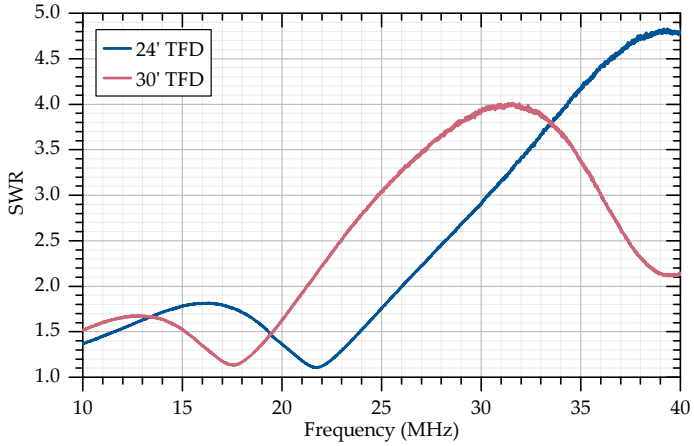

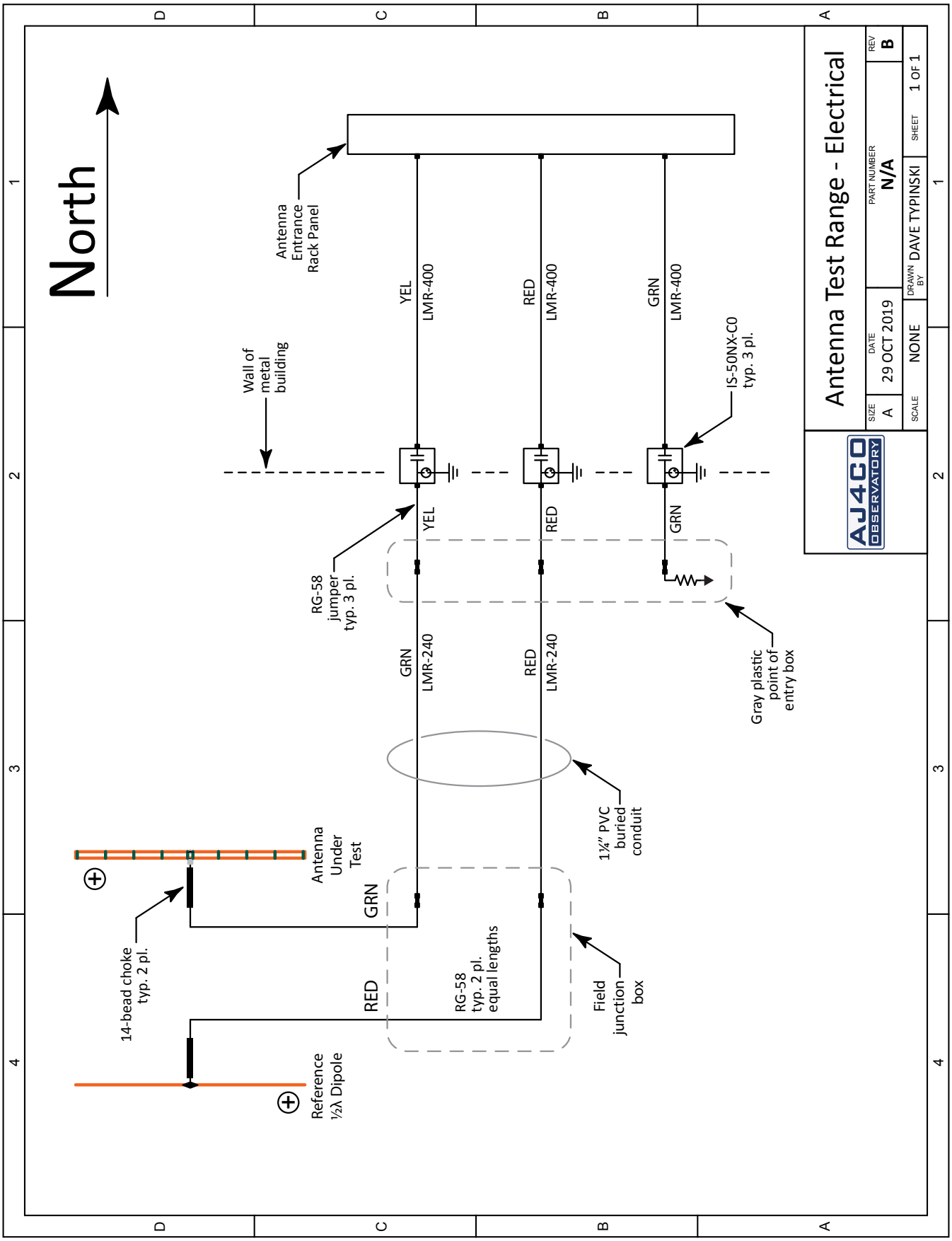
North
Antenna Entrance Rack Panel
YEL
LMR-400
RED
LMR-400
GRN
LMR-400
Wall of metal building
IS-50NX-C0 typ. 3 pl.
RG-58 jumper typ. 3 pl.
YEL
RED
GRN
GRN
LMR-240
RED
LMR-240
Gray plastic point of entry box
1¼" PVC buried conduit
Antenna Under Test
GRN
14-bead choke typ. 2 pl.
RED
RG-58 typ. 2 pl. equal lengths
Field junction box
Reference ½λ Dipole
Antenna Test Range - Electrical
AJ4CO OBSERVATORY
SIZE A
DATE 29 OCT 2019
SCALE NONE
DRAWN BY DAVE TYPINSKI
PART NUMBER N/A
SHEET 1 OF 1
REV B

Appendix 8 – Antenna Test Range Feed Losses

See Appendices 7 and 9 for locations of feed points and calibration plane.

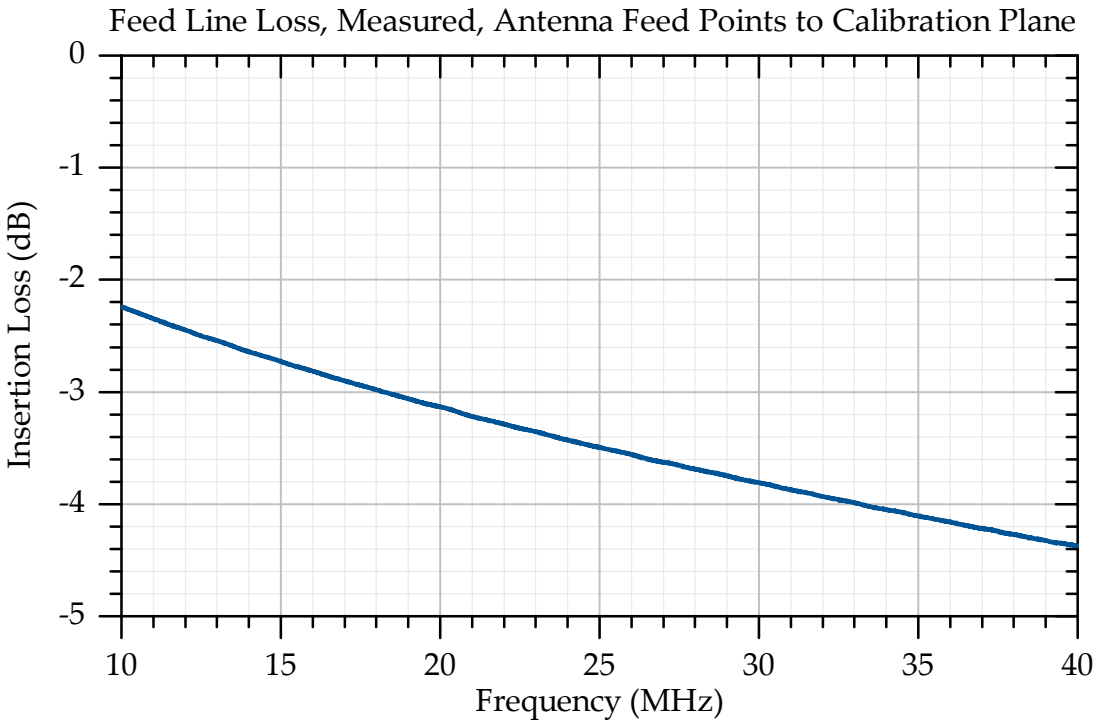

Appendix 9 – Observatory Antenna Feed Distribution

With HAT-4 pad after noise generator

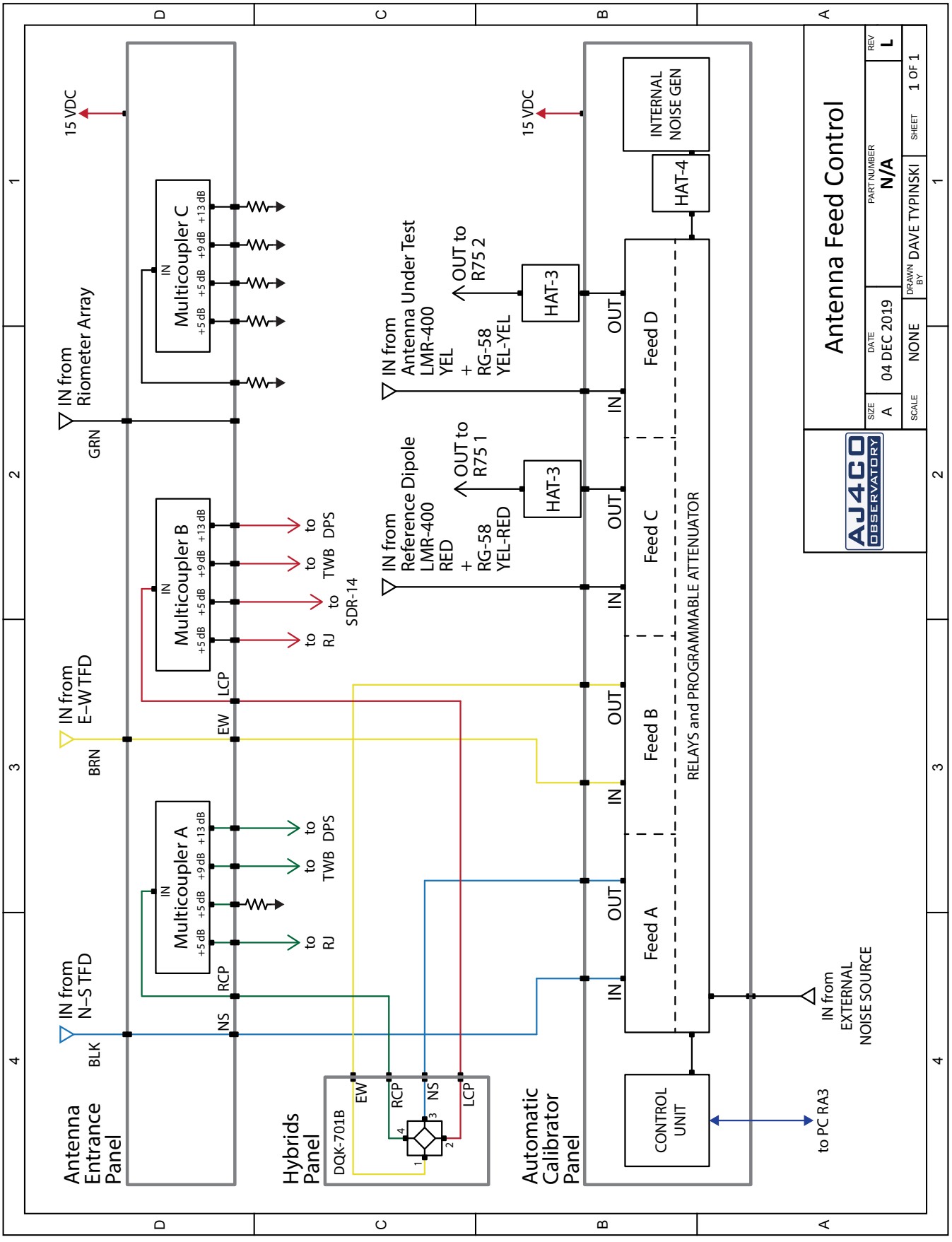

Appendix 9 – Observatory Antenna Feed Distribution

With HAT-4 and HAT-3 pads after noise generator

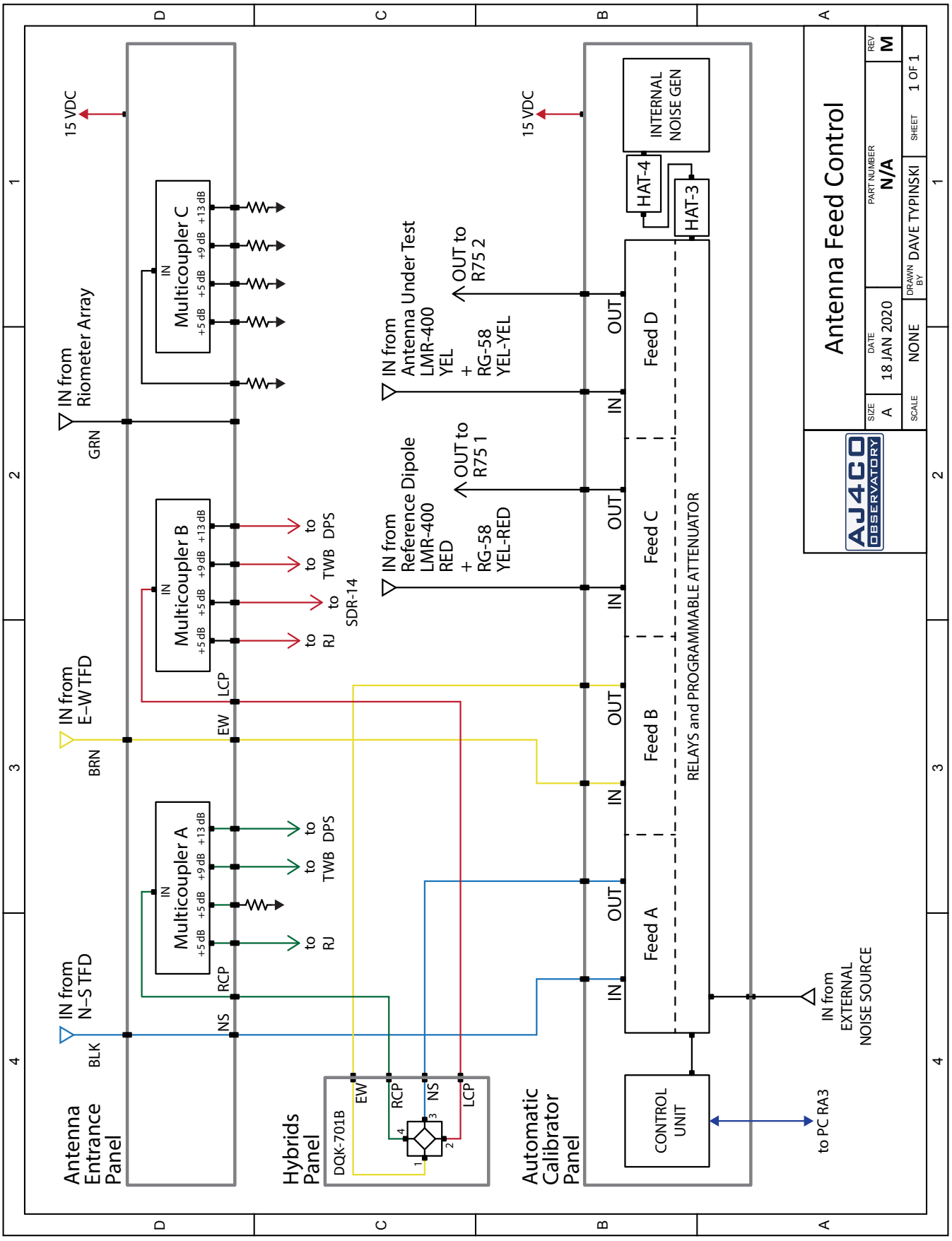

Appendix 10 – AJ4CO Automatic Calibrator Output
Measured Against 5722 on 05 Jan 2020

The AJ4CO automatic calibrator provided step calibrations. The calibrator was modified by adding a HAT-4 pad on the internal noise generator (14 through 30 MHz measurements) or HAT-4 and HAT-3 pads in series on the internal noise generator (31 through 33 MHz measurements). Plots below show the noise temperature and variation at the automatic calibrator front panel connectors (the calibration plane) during the calibrator's 0 dB attenuation step.

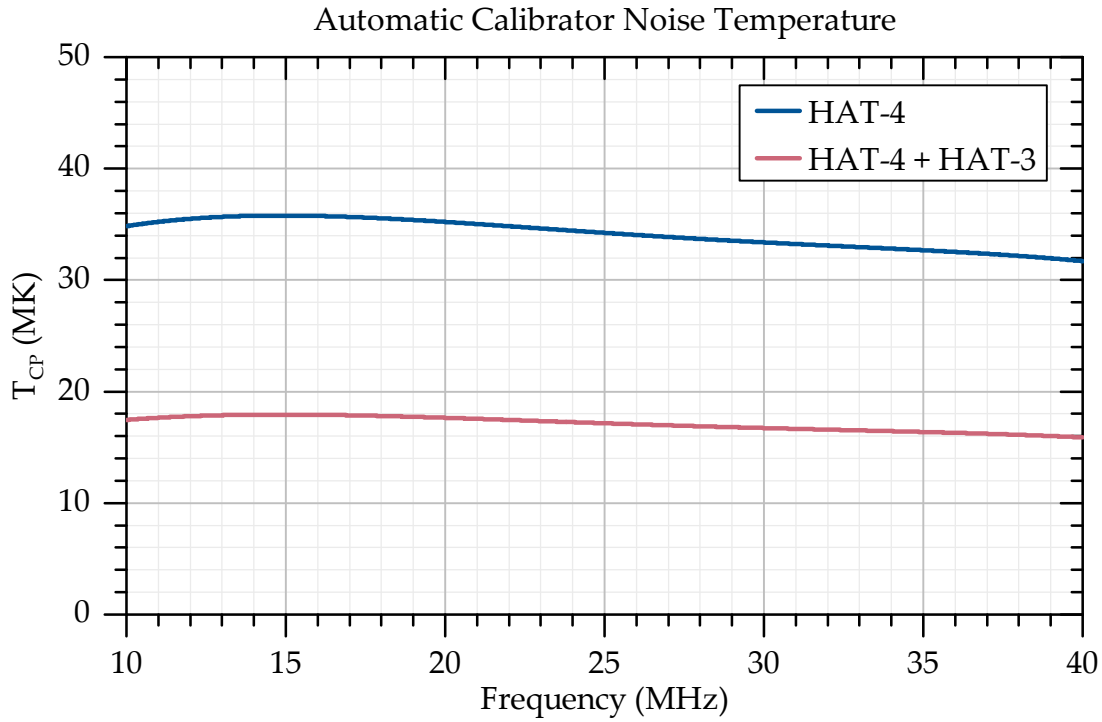

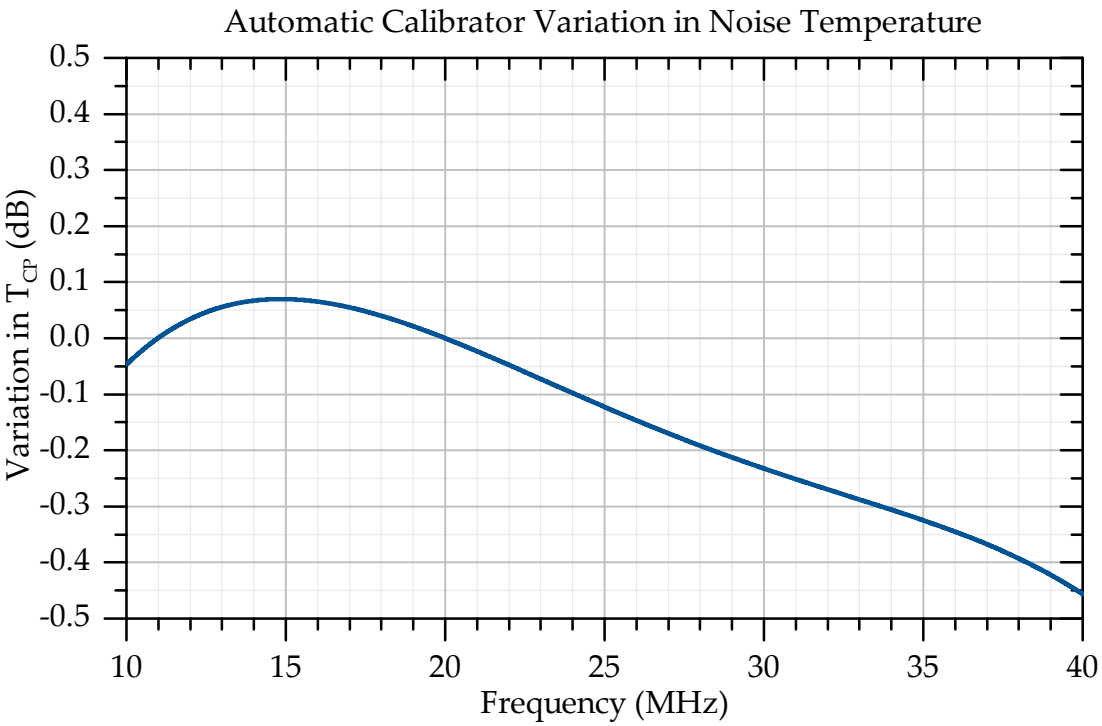

Appendix 11 – Antenna Test Range Receivers, With Preamps

See Appendix 14 for a list of the measurements that used preamplifiers and those that did not.

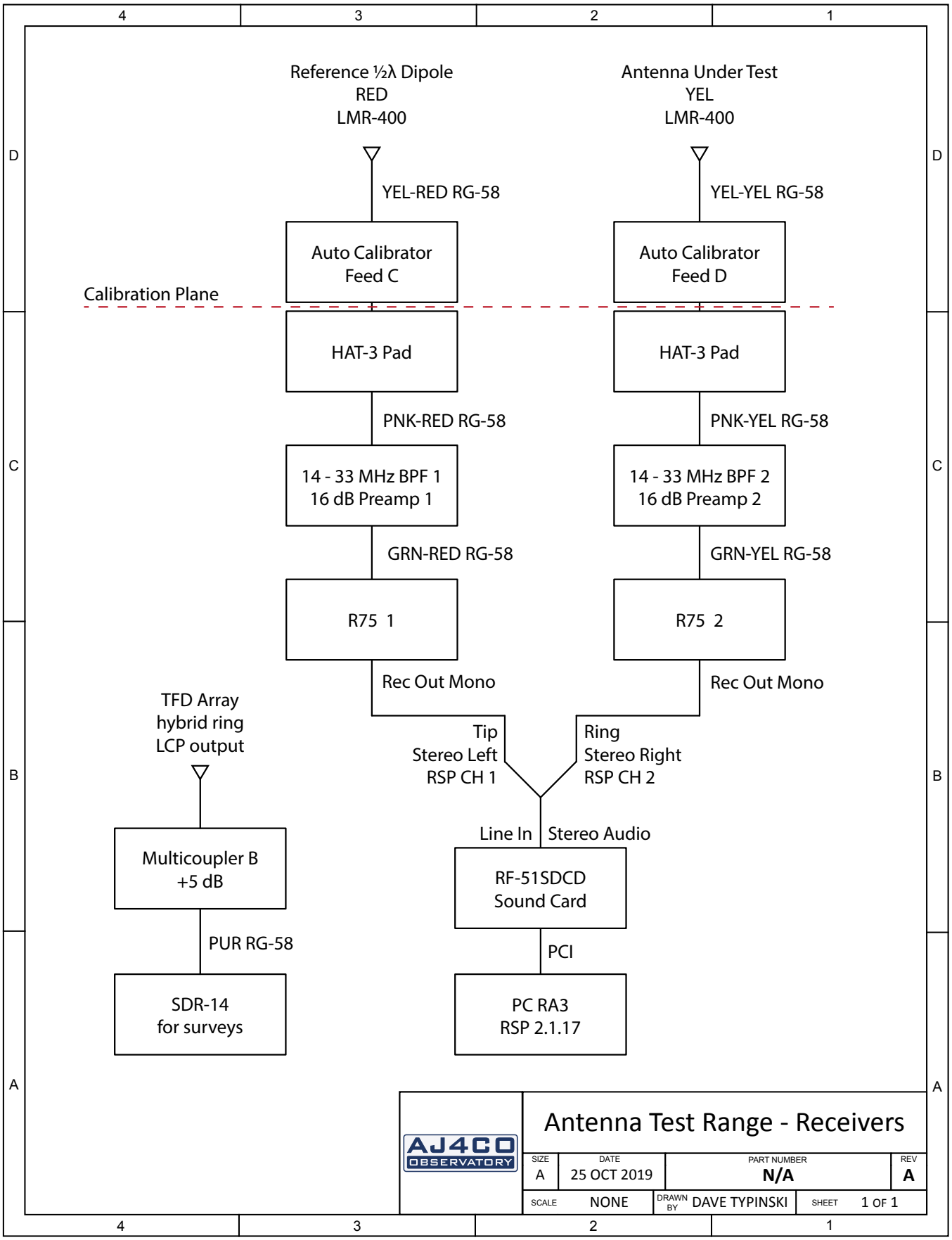

Appendix 12 – Antenna Test Range Receivers, Without Preamps

See Appendix 14 for a list of the measurements that used preamplifiers and those that did not.

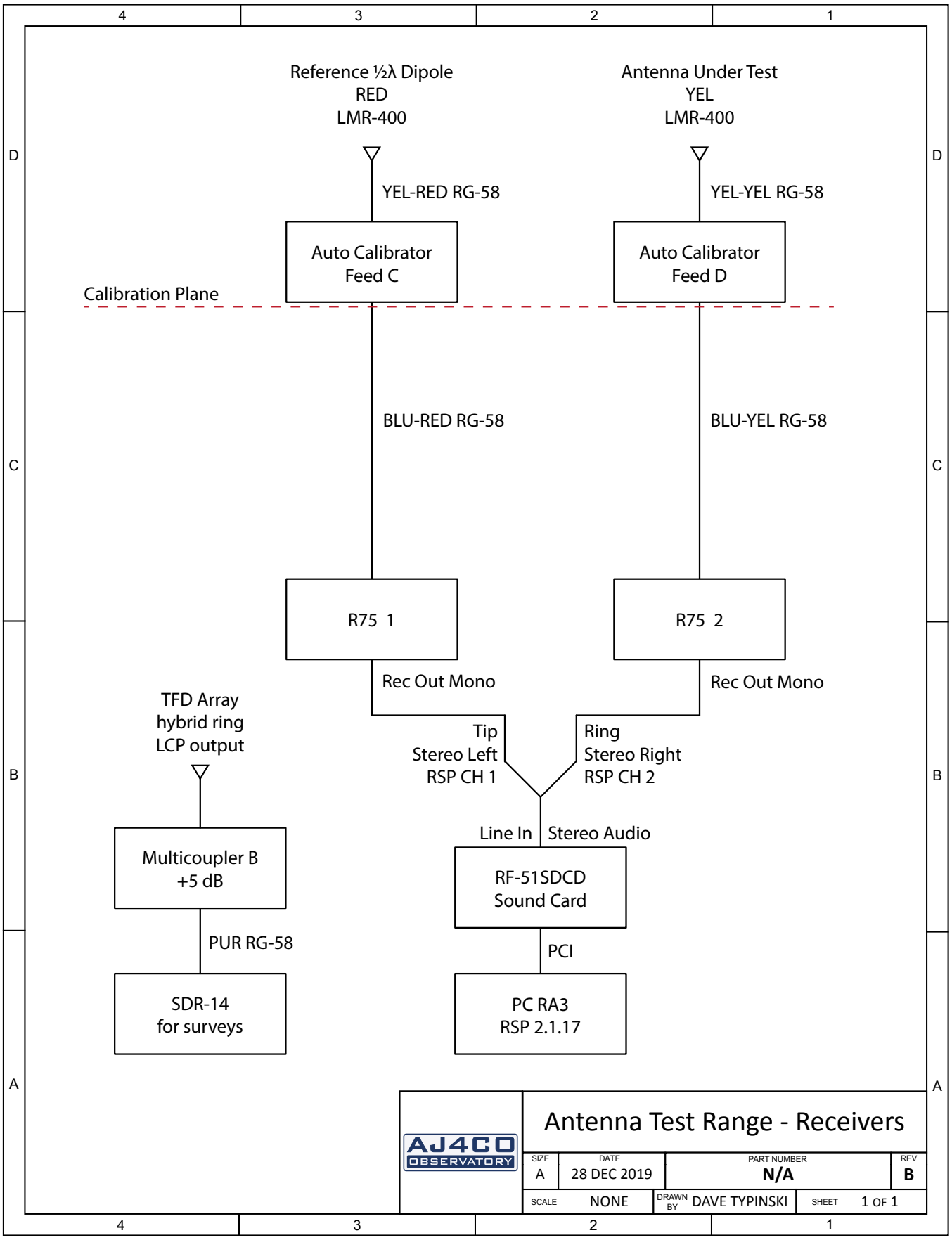

Appendix 13 – Antenna Test Range Preamp Gains

Preamp gains measured 03 Jan 2020

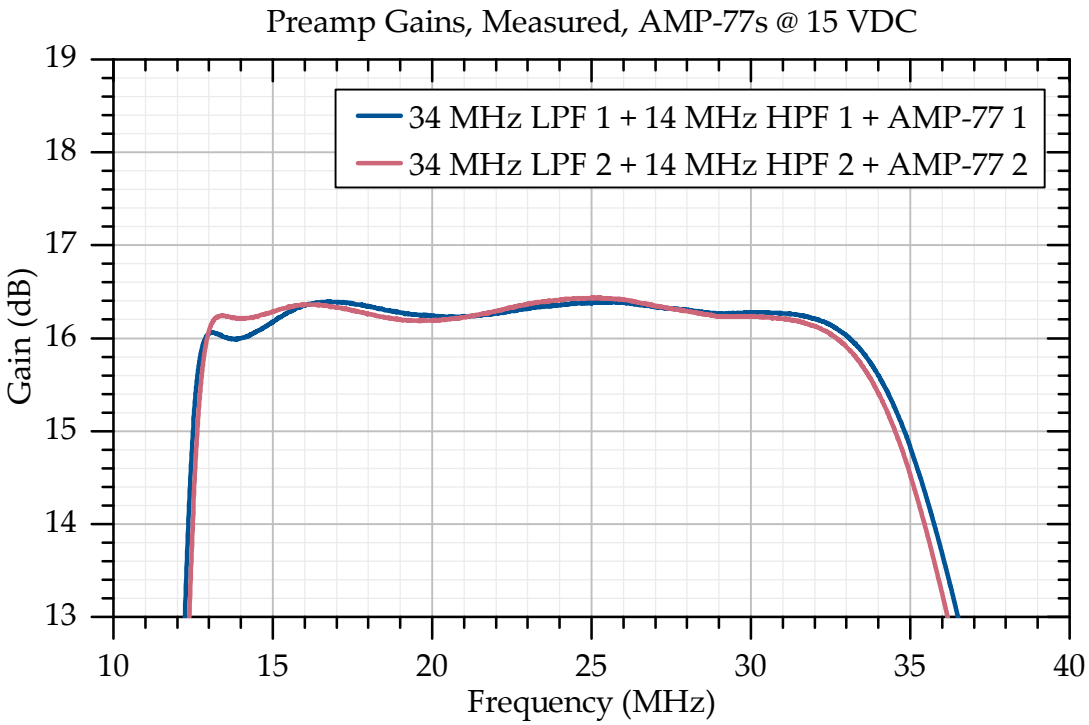

Appendix 14 – Antenna Test Log

A matched pair of preamplifiers were fabricated by RF Associates, LLC for the R75 receivers and were installed as noted in Appendix 11. Variation in amplitude on a scale of tens of minutes in the observed GB signal level created suspicion that the physical location of the preamps might be a cause. The preamp components – LPF, HPF and AMP-77 – were each enclosed in separate well-shielded aluminum boxes bolted to a 6″ square aluminum plate. However, the preamp assemblies in operation were placed on a shelf with the R75s. Neither the preamps nor the receivers had any RF grounding other than the shields of the coax cables.

The preamps were removed for the 24 MHz tests and thereafter. Time did not permit fabrication of a well-grounded rack chassis to house the preamps. Lack of preamplification does not appear to have affected the test series except at 32 and 33 MHz; but, it is unknown if the slight deviation from expected GB temperatures at these two frequencies (see Plot 2) is due to insensitivity (noise figure) of the receivers without preamps or weak RFI.

Variations in amplitude of the observed GB appeared again after removal of the preamps, but on a different charcteristic time scale. It remains unknown if the lack of RF grounding on the preamps and/or receivers caused such effects.

Date	UTC	Freq (MHz)	Preamp Gain (dB)	Notes
2019 Dec 04	1410	14.41	16	Installed 14 MHz reference dipole and 30′ TFD
2019 Dec 06	1124	14.41	16	14 MHz T30 measurement
2019 Dec 07	2242	14.41	16	Removed 30′ TFD and replaced with 24′ TFD
2019 Dec 08	0753	14.41	16	14 MHz T24 measurement
2019 Dec 08	1725	15.07	16	Trimmed reference dipole to 15 MHz
2019 Dec 09	1033	15.07	16	15 MHz T24 measurement
2019 Dec 09	2331	15.07	16	Removed 24′ TFD and replaced with 30′ TFD
2019 Dec 10	1009	15.07	16	15 MHz T30 measurement
2019 Dec 10	2258	16.08	16	Trimmed reference dipole to 16 MHz
2019 Dec 11	0939	16.08	16	16 MHz T30 measurement
2019 Dec 11	2306	16.08	16	Removed 30′ TFD and replaced with 24′ TFD
2019 Dec 12	0945	16.08	16	16 MHz T24 measurement
2019 Dec 12	2333	17.05	16	Trimmed reference dipole to 17 MHz
2019 Dec 13	1010	17.05	16	17 MHz T24 measurement
2019 Dec 13	2216	17.05	16	Removed 24′ TFD and replaced with 30′ TFD
2019 Dec 14	0218	17.05	16	17 MHz T30 measurement

Date	UTC	Freq (MHz)	Preamp Gain (dB)	Notes
2019 Dec 14	1903	18.04	16	Trimmed reference dipole to 18 MHz
2019 Dec 15	1011	18.04	16	18 MHz T30 measurement
2019 Dec 15	1918	18.04	16	Removed 30′ TFD and replaced with 24′ TFD
2019 Dec 16	1025	18.04	16	18 MHz T24 measurement
2019 Dec 17	0132	19.07	16	Trimmed reference dipole to 19 MHz
2019 Dec 17	1023	19.07	16	19 MHz T24 measurement
2019 Dec 17	1527	19.07	16	Removed 24′ TFD and replaced with 30′ TFD
2019 Dec 18	0944	19.07	16	19 MHz T30 measurement
2019 Dec 18	2201	20.05	16	Trimmed reference dipole to 20 MHz
2019 Dec 19	1022	20.05	16	20 MHz T30 measurement
2019 Dec 19	2220	20.05	16	Removed 30′ TFD and replaced with 24′ TFD
2019 Dec 20	1007	20.05	16	20 MHz T24 measurement
2019 Dec 20	2249	20.95	16	Trimmed reference dipole to 21 MHz
2019 Dec 21	1034	20.95	16	21 MHz T24 measurement
2019 Dec 21	1942	20.95	16	Removed 24′ TFD and replaced with 30′ TFD
2019 Dec 22	0943	20.95	16	21 MHz T30 measurement
2019 Dec 22	1903	22.05	16	Trimmed reference dipole to 22 MHz
2019 Dec 23	1010	22.05	16	22 MHz T30 measurement
2019 Dec 23	1714	22.05	16	Removed 30′ TFD and replaced with 24′ TFD
2019 Dec 24	1013	22.05	16	22 MHz T24 measurement
2019 Dec 24	1910	23.11	16	Trimmed reference dipole to 23 MHz
2019 Dec 25	0955	23.11	16	23 MHz T24 measurement
2019 Dec 25	2204	23.11	16	Removed 24′ TFD and replaced with 30′ TFD
2019 Dec 26	0947	23.11	16	23 MHz T30 measurement
2019 Dec 26	2321	24.10	16	Trimmed reference dipole to 24 MHz
2019 Dec 27	2220	24.10	16	Removed 30′ TFD and replaced with 24′ TFD
2019 Dec 28	2033	24.10	0	Removed preamps and 3 dB pads
2019 Dec 29	0941	24.10	0	24 MHz T24 measurement
2019 Dec 29	1829	24.10	0	Removed 24′ TFD and replaced with 30′ TFD
2019 Dec 31	0929	24.10	0	24 MHz T30 measurement

Date	UTC	Freq (MHz)	Preamp Gain (dB)	Notes
2019 Dec 31	2204	25.12	0	Trimmed reference dipole to 25 MHz
2020 Jan 01	0944	25.12	0	25 MHz T30 measurement
2020 Jan 01	1840	25.12	0	Removed 30′ TFD and replaced with 24′ TFD
2020 Jan 02	0928	25.12	0	25 MHz T24 measurement
2020 Jan 02	2252	26.05	0	Trimmed reference dipole to 26 MHz
2020 Jan 03	0907	26.05	0	26 MHz T24 measurement
2020 Jan 03	2212	26.05	0	Removed 24′ TFD and replaced with 30′ TFD
2020 Jan 04	0909	26.05	0	26 MHz T30 measurement
2020 Jan 04	1724	27.10	0	Trimmed reference dipole to 27 MHz
2020 Jan 06	0827	27.10	0	27 MHz T30 measurement
2020 Jan 05	1744	27.10	0	Removed 30′ TFD and replaced with 24′ TFD
2020 Jan 06	0827	27.10	0	27 MHz T24 measurement
2020 Jan 06	2336	28.12	0	Trimmed reference dipole to 28 MHz
2020 Jan 07	0827	28.12	0	28 MHz T24 measurement
2020 Jan 07	2235	28.12	0	Removed 24′ TFD and replaced with 30′ TFD
2020 Jan 08	0827	28.12	0	28 MHz T30 measurement
2020 Jan 08	2342	29.13	0	Trimmed reference dipole to 29 MHz
2020 Jan 09	0840	29.13	0	29 MHz T30 measurement
2020 Jan 10	0015	29.13	0	Removed 30′ TFD and replaced with 24′ TFD
2020 Jan 10	0838	29.13	0	29 MHz T24 measurement
2020 Jan 11	0005	30.07	0	Trimmed reference dipole to 30 MHz
2020 Jan 11	0827	30.07	0	30 MHz T24 measurement
2020 Jan 12	0436	30.07	0	Removed 24′ TFD and replaced with 30′ TFD
2020 Jan 13	0822	30.07	0	30 MHz T30 measurement
2020 Jan 14	2223	30.07	0	Removed 30′ TFD and replaced with 24′ TFD
2020 Jan 16	2306	31.10	0	Trimmed reference dipole to 31 MHz
2020 Jan 18	0149	31.10	0	Removed 24′ TFD and replaced with 30′ TFD
2020 Jan 19	0826	31.10	0	31 MHz T30 measurement
2020 Jan 20	0141	31.10	0	Removed 30′ TFD and replaced with 24′ TFD
2020 Jan 20	0820	31.10	0	31 MHz T24 measurement

Date	UTC	Freq (MHz)	Preamp Gain (dB)	Notes
2020 Jan 20	2247	32.10	0	Trimmed reference dipole to 32 MHz
2020 Jan 21	0730	32.10	0	32 MHz T24 measurement
2020 Jan 21	1713	32.10	0	Removed 24′ TFD and replaced with 30′ TFD
2020 Jan 23	0730	32.10	0	32 MHz T30 measurement
2020 Jan 23	2302	33.10	0	Trimmed reference dipole to 33 MHz
2020 Jan 24	0720	33.10	0	33 MHz T30 measurement
2020 Jan 24	2147	33.10	0	Removed 30′ TFD and replaced with 24′ TFD
2020 Jan 25	0720	33.10	0	33 MHz T24 measurement